36, 466 (1972); 39, 657 (1974)].
[3]V. D. Borman, L. A. Maksimov, B. I. Nikolaev, and V. I. Troyan, Zh. Eksp. Teor. Fiz. 64, 526 (1973) [Sov. Phys. JETP 37, 269 (1973)].
[4]S. Yu. Krylov, V. D. Borman, B. I. Nikolaev, and V. I. Troyan, Zh. Eksp. Teor. Fiz. 67, 2122 (1974) [Sov. Phys. JETP 40, 1053 (1975)].
[5]V. D. Borman, B. I. Buttsev, S. Yu. Krylov, B. I. Nikolaev, and V. I. Troyan, Zh. Eksp. Teor. Fiz. 70, 929 (1976) [Sov. Phys. JETP 43, 484 (1976)].
[6]V. D. Borman, B. I. Nikolaev, and V. A. Ryabov, Zh. Eksp. Teor. Fiz. 67, 1377 (1974) [Sov. Phys. JETP 40, 684 (1975)].
[7]L. L. Gorelik, Yu. N. Redkoborodyĭ, and V. V. Spnitsyn, Zh. Eksp. Teor. Fiz. 48, 761 (1965) [Sov. Phys. JETP 21, 503 (1965)].
[8]L. J. F. Hermans, J. M. Koks, A. F. Hengeveld, and H. F. D. Knaap, Physica 50, 410 (1970).
[9]J. J. M. Beenakker and F. R. McCourt, Ann. Rev. Phys. Chem. 21, 47 (1970).
[10]G. G. Scott, G. W. Smith, and D. L. Fry, Phys. Rev. A 2, 2080 (1970).
[11]L. A. Maksimov, Zh. Eksp. Teor. Fiz. 61, 604 (1971) [Sov. Phys. JETP 34, 322 (1971)].
[12]C. Cercignani, Mathematical Methods in the Kinetic Theory of Gases, Plenum Press, New York, 1969 (Russ. Transl., Mir, M., 1972).

Translated by S. Chomet

Structure of a transverse shock wave in a plasma

A. L. Velikovich and M. A. Liberman

Institute of Physics Problems, USSR Academy of Sciences
(Submitted April 13, 1976)
Zh. Eksp. Teor. Fiz. 71, 1390–1411 (October 1976)

The structure of a shock wave front propagating in a fully ionized collision-dominated plasma perpendicular to the direction of the magnetic field is determined for arbitrary values of $\beta = 8\pi p/H^2$. It is shown that in the case of a magnetized plasma ($\Omega_i\tau_i > 1$) the wave front structure is determined by the ion viscosity and by the dispersion due to inertia of the electrons. The dispersion is more important at small values of β, and the structure of the wave front consists of oscillations that decay behind the wave front. At finite values of β the shock wave front is monotonic. In a shock wave with a sufficiently big temperature discontinuity, however, dispersion predominates at the beginning of the front and leads to the appearance of decaying oscillations ahead of the shock wave front. The Alfvén Mach numbers that are critical for the effect of dispersion are found. Dispersion due to electron inertia is not essential in the case of an unmagnetized plasma ($\Omega_e\tau_e < 1$). The width of the shock wave front is determined by Joule dissipation. The values of the critical Mach number ($M_a^h(\beta)$ above which Joule dissipation is insufficient for a continuous transition from a state ahead of the shock wave front to a state behind it are found. An isomagnetic discontinuity is produced behind the shock wave front in this case. The structure of the isomagnetic discontinuity, which is determined by the electron thermal conductivity, ion viscosity, and ion thermal conductivity, is found.

PACS numbers: 52.35.Lv

The structure of transverse shock waves in a plasma has been the subject of many theoretical as well as experimental studies (see, e.g., the review[1] and the book[2]). In view of the great variety of interactions of particles in the plasma, the structure of the shock wave is determined by various dissipative processes or dispersion effects, depending on the magnetic field strength and on the relations between the plasma parameters.

The first studies of shock waves in plasma[3,4] yielded only a qualitative picture of the structure of the shock-wave front in the limit of a strong shock wave and under the assumption that the wavefront is the result of ion viscosity. The authors of subsequent papers devoted to the structure of the front of collision shock waves limited themselves either to numerical calculations or arbitrarily left in the equations a dissipation of some sort, neglecting the dispersion and the remaining dissipative terms.[5–9] Naturally, the region of applicability of the results obtained in this manner is not clear.

A number of studies[10–12] yielded the values of the critical Mach numbers which specify the boundary above which there exists no integral curve joining the states ahead and behind the shock-wave front.

In the present paper, the critical Mach numbers are obtained for arbitrary values of β. It is shown that the boundary shock-wave intensities defined by these numbers signify either that at high intensity the chosen principal dissipation is insufficient for the formation of the shock front, or that oscillations appear on the front as a result of predominance of dispersion at an intensity below the given value.[13,14]

The magnetic field in the plasma is usually characterized by the ratio $\beta = 8\pi p/H^2$ of the gas pressure to the magnetic-field pressure. Collisionless shock waves correspond to the cold-plasma limit, i.e., $\beta \ll 1$. A more convenient parameter when using the structure of shock waves is the degree of plasma magnetization $\Omega\tau$, where $\Omega_{e,i} = eH/m_{e,i}c$ is the cyclotron (electron) frequency and

$$\tau_{e,i}=3m_{e,i}^{1/2}T_{e,i}^{3/2}/4\pi^{1/2}\lambda e^4 n$$

is the corresponding time of the Coulomb collisions. It turns out that the dispersion due to electron inertia can be significant only in a magnetized plasma.

The principal dissipative process in a magnetized plasma is always the ion viscosity,[15] but at small values of β a more important role is assumed by dispersion, and the structure of the shock-wave front (for example, the change of the magnetic field) constitutes in this case oscillations that are damped behind the shock-wave front. In the case of a large temperature jump, the oscillations can be produced also ahead of the shock-wave front. We obtain in this paper the critical values of the Mach numbers $M_a(\beta)$, below which oscillations on the front are possible.

In the case of a partially magnetized or unmagnetized plasma ($\Omega_i \tau_i < 1$), the dispersion due to electron inertia is suppressed by the Joule dissipation and does not influence the structure of the wave front, which is determined mainly by the plasma resistance. But the Joule dissipations cannot form a front of an arbitrary strong shock wave, and therefore a discontinuity of the type of the isothermal jump appears in the structure at an intensity above a certain value.[11,16-19] Thus, in the case of shock waves with $M_a > M_a^h(\beta)$ ($M_a^h = 2.76$ at $\beta \ll 1$) an internal discontinuity appears on the shock-wave front, namely an isomagnetic jump, in which a discontinuity appears in the velocity, density, temperature, etc. at an almost constant magnetic field.

The width of this discontinuity is determined by the electronic thermal conductivity. On the other hand, when the intensity of the shock wave is even larger, $M_a > M_a^T(\beta)$ ($M_a^T = 3.02$ at $\beta \ll 1$), the velocity and the density experience inside the isomagnetic jump one more discontinuity at a constant electron temperature. The width of the latter discontinuity—the electron isothermal jump—is determined already by the ion viscosity.

We note that although formally the value of the critical Alfvén Mach number M_a^h as $\beta \to 0$ is the same in a collision-dominated plasma as for the isomagnetic jump in a collisionless shock wave,[20-22] their physical natures are entirely different.

1. We consider a stationary plane shock wave propagating in a fully ionized plasma along the x axis. We direct the z axis along the magnetic H. We assume the plasma to be simple with $\gamma_e = \gamma_i = \frac{5}{3}$. As usual, we change over to a coordinate system moving together with the shock-wave front. In this system, the plasma flows in from $x = -\infty$ in state 1 and flows out to $x = +\infty$ in state 2—behind the front of the shock wave. Considering a planar stationary problem, we obtain for the y component of the electric field, from the equation $\operatorname{curl}\mathbf{E} = 0$, that E_y is constant. The boundary conditions at $\pm\infty$ yield $E_y = u_1 H_1/c = u_2 H_2/c$. The subscripts 1 and 2 pertain here to states far in front ($x = -\infty$) and far behind ($x = +\infty$) the shock-wave front, respectively. We shall neglect the dispersion effects due to deviation from quasineutrality, assuming in first-order approximation that $n_i = n_e = n$, $r_D = 0$ and determining the critical field E_x in the next-order approximation in r_D. We then obtain from the equation $\operatorname{curl}\mathbf{H} = 4\pi\mathbf{j}/c$

$$\frac{dH}{dx} = \frac{4\pi}{c} ne(v_y^e - v_y^i). \tag{1.1}$$

The vanishing of the x component of the current together with the quasineutrality condition yields $v_x^i = v_x^e = v$.

As the material equations for the collision-dominated plasma we choose the equations of two-fluid hydrodynamics for the electrons and ions and the values of the kinetic coefficients obtained by Braginskiĭ.[23]

We write down the first integrals of the equations for the continuity and for the conservation of the momentum and energy fluxes for the entire plasma as a unit in the form

$$nv = C; \tag{1.2}$$

$$(m_e + m_i)Cv + n(T_e + T_i) + \pi_{xx}^e + \pi_{xx}^i + \frac{H^2 - E_x^2}{8\pi} = P; \tag{1.3}$$

$$(m_e v_y^e + m_i v_y^i)C + \pi_{xy}^e + \pi_{xy}^i - \frac{E_x E_y}{4\pi} = G; \tag{1.4}$$

$$\frac{m_e}{2}(v^2 + v_y^{e2})C + \frac{m_i}{2}(v^2 + v^{i2})C + \frac{5}{2}(T_e + T_i)C + \pi_{x\beta}^e v_\beta^e + \pi_{x\beta}^i v_\beta^i + q_x^e + q_x^i + \frac{c}{4\pi} E_y H = S, \tag{1.5}$$

where C, P, G, and S are integration constants determined from the boundary conditions.

Equations (1.2)–(1.5) must be supplemented with the equations of motion and the thermal conductivity for the electrons

$$m_e C \frac{dv}{dx} + \frac{d}{dx} nT_e + \frac{d}{dx}\pi_{xx}^e + enE_x + \frac{e}{c} nv_y^e H = R_x; \tag{1.6}$$

$$m_e C \frac{dv_y^e}{dx} + \frac{d}{dx}\pi_{xy}^e + enE_y - \frac{e}{c} nvH = R_y; \tag{1.7}$$

$$\frac{3}{2} C \frac{dT_e}{dx} + nT_e \frac{dv}{dx} + \frac{d}{dx} q_x^e + \pi_{xx}^e \frac{dv}{dx} + \pi_{xy}^e \frac{dv_y^e}{dx} = Q_e. \tag{1.8}$$

Here $T_{i,e}$, $\pi_{\alpha\beta}^{i,e}$, $\mathbf{q}_{i,e}$ are respectively the temperatures, viscous-stress tensors, and heat fluxes of the ions and the electrons; R_x and R_y are the components of the friction force acting between the ions and the electrons; Q_e is the heat obtained when the electrons collide with the ions.

The investigation and solution of Eqs. (1.1)–(1.8) is preferably carried out by changing over to dimensionless variables. We introduce the dimensionless temperatures, velocities, densities, etc. as ratios of their values to the corresponding equilibrium values in states 1 or 2, i.e., ahead or behind the shock-wave front. The dimensionless variables E and Φ (the x component of the electric field and the electrostatic potential) are the ratios of the corresponding energies to the thermal energy in the equilibrium state. Finally, the scale Δ of the coordinate x should be specially determined from physical considerations. Referring all quantities, for example, to the state 2, we denote

$$\omega = v/u_2,\ \lambda_{i,e} = v_y^{i,e}/u_2,\ \nu = n/n_2,\ \Theta_{i,e} = T_{i,e}/T_2,\\ h = H/H_2,\ E = eE_x r_{D_2}/T_2,\ \Phi = e\varphi/T_2,\ \zeta = x/\Delta. \tag{1.9}$$

It is known that only one fast magnetosonic wave propagates across the magnetic field, with velocity $\tilde{u} = (u_s^2 + u_a^2)^{1/2}$, where u_s is the velocity of ordinary sound and u_a is the velocity of the Alfvén wave. Thus, by defining the Mach number as the ratio of the flux velocity to the velocity of the fast magnetosonic wave, $\mathscr{M} = u/\tilde{u}$, we have $\mathscr{M}_1 > 1$ for the transverse shock wave (supersonic flux). We introduce as the parameter of the dimensionless equations not the number $\mathscr{M}$, but the acoustic and Alfvén Mach numbers $M = u/u_s$ and $M_a = u/u_a$, respectively, which are connected with $\mathscr{M}$ by the simple relation

$$\mathscr{M} = MM_a/(M^2+M_a^2)^{1/2}. \tag{1.10}$$

The region of variation of the numbers M and M_a in the incoming flux, corresponding to the shock wave, is shown in Fig. 1—this is the region above the hyperbola $M_1^{-2}+M_{a_1}^{-2}=1$ on the $(M_1^2, M_{a_1}^2)$ plane.

Written in terms of the dimensionless quantities behind the shock-wave front, the equations contain the Mach numbers M_2 and M_{a_2} in the outgoing flux, which are connected with M_1 and M_{a_1} by the relation[15]

$$M_2^2 = M_1^2\omega_2^2/\Theta_2, \quad M_{a_2}^2 = M_{a_1}^2\omega_2^3, \tag{1.11}$$

where ω_2 and Θ_2 are the jumps in the velocity and in the temperature through the shock-wave front

$$\omega_2 = \frac{1}{\omega_1} = \frac{u_2}{u_1} = \frac{1}{8}\left\{1+\frac{3}{M_1^2}+\frac{5}{2M_{a_1}^2}+\left[\left(1+\frac{3}{M_1^2}+\frac{5}{2M_{a_1}^2}\right)^2+\frac{8}{M_{a_1}^2}\right]^{1/2}\right\}. \tag{1.12}$$

$$\Theta_2 = \frac{1}{\Theta_1} = \frac{T_2}{T_1} = 1+M_1^2(1-\omega_2)\left(\omega_2^2+\omega_2-\frac{2}{M_{a_1}^2}\right)\Big/3\omega_2. \tag{1.13}$$

The region of variation of the numbers M_2 and M_{a_2}, corresponding to the shock wave, i.e., to the condition $\mathscr{M}_1 > 1$ is shown in Fig. 2. On the $(M_2^2, M_{a_2}^2)$ plane it is located between the hyperbola $M_2^{-2}+M_{a_2}^{-2}=1$ and a curve whose parametric equation is

$$M_2^2 = \frac{3\omega_2^2(5\omega_2+1)}{5(1-\omega_2)^3}, \quad M_{a_2}^2 = \frac{\omega_2^2(5\omega_2+1)}{2(4\omega_2-1)}.$$

In Fig. 2 the upper boundary—the hyperbola—corresponds to the limit of the weak shock wave ($\omega_2 = 1$, $\Theta_2 = 1$), while the lower one corresponds to the limit $M_1 \to \infty$, i.e., to an infinitely large temperature jump at an arbitrary compression ω_2. In particular, at sufficiently large M_2 (small $\beta_2 = \frac{6}{5}M_{a_2}^2/M_2^2$) there are realized shock waves in which an arbitrarily large temperature jump is associated with an arbitrarily small compression.

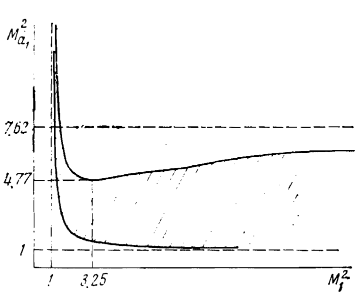

FIG. 1. The values of the Mach numbers corresponding to the shock wave, i.e., $\omega_2 < 1$, lie above the hyperbola $M_1^{-2}+M_{a_1}^{-2}=1$. The region $M_2 > 1$, in which the shock wave can have a nonmonotonic structure, is shown shaded. $M_a(\beta=0) = 2.76$.

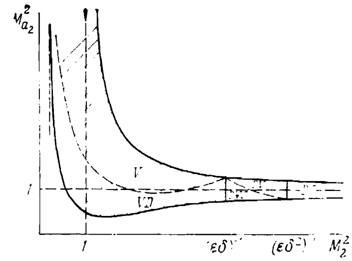

FIG. 2. Region, corresponding to $\omega_1 > 1$, of the Mach numbers behind the front of the shock wave.

We put $\varepsilon = (m_e/m_i)^{1/2}$ and denote the degree of magnetization of the ions by $(\Omega_i\tau_i)^{-1} = r_i/l_i = \delta$. Then $(\Omega_e\tau_e)^{-1} = \varepsilon\delta$.

Since the form of the equation and the values of the kinetic coefficients are different and depend on the value of δ, we consider separately two limiting cases, $\delta \ll 1$ and $\varepsilon\delta \gg 1$. Inasmuch as the temperature increases through the shock-wave front it follows that, assuming $\delta \ll 1$ ahead of the shock-wave front, we see that the first inequality (the condition of strong magnetization) is not violated also behind the front. To the contrary, the second inequality (the condition of weak magnetization) can be satisfied ahead of the shock-wave front and is violated behind it at sufficiently large intensities. This restricts the investigation of this limiting case to shock waves that are not too strong.

2. We consider a strongly magnetized plasma, in which the electrons and ions ahead of the shock-wave front are magnetized: $\delta \ll 1$ and $\varepsilon\delta \ll 1$.

In terms of the dimensionless variables (1.9), Eq. (1.1) takes the form

$$\lambda_e - \lambda_i = 1.05\frac{M_2\delta l_2}{M_{a_2}^2\Delta}\omega\frac{dh}{d\zeta}. \tag{2.1}$$

Changing over in (1.2)–(1.8) to the dimensionless variables (1.9), eliminating the y component of the dimensionless electron velocity λ_e, and omitting the small terms with electron viscosity, we obtain

$$\nu\omega = 1, \tag{2.2}$$

$$\omega - 1 + \frac{3}{10M_2^2}\left(\frac{\Theta_e+\Theta_i}{\omega}-2\right)+\frac{h^2-1}{2M_{a_2}^2}-\frac{\Delta_v}{\sqrt{10}\,\Delta}\times\left[(0.32\Theta_i^{5/2}+0.3\delta^2h^{-2}\omega^{-2}\Theta_i^{-1/2})\frac{d\omega}{d\zeta}+0.5\delta h^{-1}\omega^{-1}\Theta_i\frac{d\lambda_i}{d\zeta}\right]=0, \tag{2.3}$$

$$\frac{\omega^2-1}{2}+\frac{\lambda_i^2}{2}+\frac{3}{4M_2^2}(\Theta_i+\Theta_e-2)+\frac{h-1}{M_{a_2}^2}+1.05\frac{\varepsilon\Delta_d}{M_{a_2}^2\Delta}\lambda_i\omega\frac{dh}{d\zeta}+\frac{0.55}{M_{a_2}^2}\left(\frac{\Delta_d}{\Delta}\right)^2\left(\omega\frac{dh}{d\zeta}\right)^2-\frac{\Delta_v}{\sqrt{10}\,\Delta}\left[0.32\Theta_i^{5/2}\omega\frac{d\omega}{d\zeta}\right.$$
$$\left.+0.3\delta^2h^{-2}\omega^{-2}\Theta_i^{-1/2}\left(\omega\frac{d\omega}{d\zeta}+\lambda_i\frac{d\lambda_i}{d\zeta}\right)+0.5\delta h^{-1}\omega^{-1}\Theta_i\left(\omega\frac{d\lambda_i}{d\zeta}-\lambda_i\frac{d\omega}{d\zeta}\right)\right]$$
$$-\frac{0.47}{M_2^2}\left(\frac{\Delta_j}{\Delta}\right)\omega^{-1}\Theta_e^{-1/2}\frac{dh}{d\zeta}-\frac{0.44M_{a_2}^2}{M_2^2}\left(\frac{\Delta_j}{\Delta}\right)\omega^{-2}\Theta_e^{-1/2}\frac{d\Theta_e}{d\zeta}$$
$$-0.19\frac{\delta^2l_2}{M_2^3\Delta}h^{-2}\omega^{-2}\Theta_i^{-1/2}\frac{d\Theta_i}{d\zeta}=0, \tag{2.4}$$

$$h\omega-1=1.1\left(\frac{\Delta_d}{\Delta}\right)^2\omega\frac{d}{d\zeta}\omega\frac{dh}{d\zeta}+1.05\varepsilon M_{a_2}\frac{\Delta_d}{\Delta}\omega\frac{d\lambda_i}{d\zeta}+1.05\frac{\Delta_j}{\Delta}\Theta_e^{-1/2}\frac{dh}{d\zeta}+\frac{0.47M_{a_2}^2}{M_2^2}\left(\frac{\Delta_j}{\Delta}\right)\omega^{-1}\Theta_e^{-1/2}\frac{d\Theta_e}{d\zeta}. \tag{2.5}$$

$$\frac{d\Theta_e}{d\zeta}+\frac{2}{3}\frac{\Theta_e}{\omega}\frac{d\omega}{d\zeta}+1.1\frac{\Delta}{\Delta_r}\omega^{-2}\Theta_e^{-3/2}(\Theta_e-\Theta_i)-\frac{d}{d\zeta}\Big[1.05\frac{\Delta_j}{\Delta}h^{-1}\omega^{-1}\Theta_e^{-1/2}\frac{dh}{d\zeta}$$
$$+\frac{0.98}{M_2^2}\frac{\Delta_j}{\Delta}h^{-2}\omega^{-2}\Theta_e^{-1/2}\frac{d\Theta_e}{d\zeta}\Big]-0.17M_2^2\varepsilon\frac{\Delta_v}{\Delta}\left(\frac{d\omega}{d\zeta}\right)^2$$
$$-2.34\frac{M_2^2}{M_{c2}^2}\frac{\Delta_j}{\Delta}\Theta_e^{-3/2}\left(\frac{dh}{d\zeta}\right)^2-1.05\frac{\Delta_j}{\Delta}h^{-1}\omega^{-1}\frac{dh}{d\zeta}\frac{d\Theta_e}{d\zeta}=0, \quad (2.6)$$
$$\lambda_i-0.1\delta^2\frac{\Delta_v}{\Delta}h^{-2}\omega^{-2}\Theta_i^{-1/2}\frac{d\lambda_i}{d\zeta}+0.16\delta\frac{\Delta_v}{\Delta}h^{-1}\omega^{-1}\Theta_i\frac{d\omega}{d\zeta}=0. \quad (2.7)$$

In Eqs. (2.3)–(2.7), Δ_n stands for combinations of parameters with dimensions of length, which are characteristic of the various processes. The ion viscosity corresponds to the scale $\Delta_v = l/M$, the electron inertia corresponds to $\Delta_d = \varepsilon\delta Ml/M_a$, the Joule losses to $\Delta_j = \varepsilon\delta^2 Ml/M_a^2$, and the transfer of energy from the electrons to the ions as a result of collisions to $\Delta_r = Ml/\varepsilon$. The scale Δ of the transition to the dimensionless coordinate has so far not been defined. In the system of ordinary differential equations (2.1)–(2.7), the derivatives contain factors in the form of the ratio of the scale of the given physical process to the scale of the dimensionless coordinate. If we neglect all the derivatives, i.e., if we regard the shock wave as a discontinuity of all the quantities from the state 1 ahead of the shock-wave front to the state 2 behind the front, putting formally $\Delta = \infty$, then we arrive at the Hugoniot–Rankine relation, namely, we obtain algebraic equations that connect the values of the variables ahead and behind the shock-wave front. Solving these equations we obtain, as was done earlier,[15] the jumps of the velocity, temperature, etc. expressed in terms of the Mach numbers. On the other hand, if we are interested in the structure of the shock-wave front, then we must choose a finite value of Δ and solve the system of differential equations. Assume that all the dimensionless variables are of the order of unity, as is the case in a weak shock wave. Choosing among them the maximum parameter, say Δ_1, we put $\Delta = \Delta_1$ and neglect small terms of order Δ_n/Δ_1. We can then obtain the solutions of the initial equations in quadratures, with the dissipative process with characteristic scale Δ_1 being the decisive one for the structure of the front, and the root of the front being of the order Δ_1. If the obtained solution does not give a continuous transition from the state 1 to the state 2, then it is necessary to introduce at the discontinuity a smaller scale, etc.

The indicated program calls for certain refinements. First, there are two possibilities of going over to dimensionless variables: relative to the state 2 behind the shock-wave front and relative to the state 1 ahead of the shock-wave front. As shown earlier,[15] the velocities, concentrations, and the magnetic field in the shock wave vary in finite limits, i.e., the magnetic field in the shock wave vary in finite limits, i.e., their dimensionless values are always of the order of unity. However, the temperature jump even in a weak shock wave (at small β) can be arbitrarily large. The two possibilities of changing to dimensionless variables relative to the values of variables of states 1 and 2 afford two choices of scales characterizing the given physical process. For example, the scale characterizing the isotropic component of the ion viscosity can be chosen the form $\Delta_v(1) = l_1/M_1$ or $\Delta_v(2) = l_2/M_2$. In order of magnitude we have $\Delta_v(1)/\Delta_v(2) \approx \Theta_1^{5/2}$. Since the boundary conditions admit of an arbitrary value $0 < \Theta_1 < 1$, it follows that $\Delta_v(1)$ can be arbitrarily small in comparison with $\Delta_v(2)$. The physical cause of this is precisely the fact that the action of the viscosity increases in proportion to $T^{5/2}$.

Thus, in order for any one particular physical process to predominate over the extent of the entire shock-wave layer, it is necessary that the length scale which is characteristic of this process, be the largest everywhere. In the opposite case it is necessary to take into account the competing processes in one or another section of the shock layer. It must also be borne in mind that Δ is not necessarily of the order of the width of the shock-wave front. Weak shock waves are broader. To estimate the width of the front of a weak shock wave we introduce the shock-wave intensity $I = 1 - \mathscr{M}_1^{-2}$. This parameter varies between 0 and 1 (corresponding to the limits of infinitesimally weak and infinitely strong shock wave respectively). The solution for the weak shock wave ($I \ll 1$) is

$$\omega = 1 + AI[1 + \operatorname{th}(AI\zeta)],$$

where $A = (9+5\beta_1)/2(9+20\beta_1/3)$, from which it follows that the width of a weak shock wave is of the order of $\Delta/I \gg \Delta$.

In Eqs. (2.3)–(2.7) we can separate the following processes and the scales corresponding to them: $\Delta_v = l/M$ corresponds to ion viscosity and has a maximum value behind the shock-wave front in state 2. $\Delta_d = \varepsilon\delta Ml/M_a$ corresponds to the dispersion due to the electron inertia. It is easy to verify that $\Delta_d = c/\omega_p$ is the collisionless skin depth. Naturally, over $\Delta = \Delta_d$ the freezing-in of the magnetic field is violated. $\Delta_j = \varepsilon\delta^2 Ml/M_a^2$ corresponds to the Joule losses and to the Hall fluxes; $\Delta_r = Ml/\varepsilon$ is the scale of the temperature relaxation of the electron and ions. From a comparison of these four scales we see that the largest of them is always Δ_r. But the energy exchange between the electrons and ions can by itself not give rise to a shock wave.

As shown earlier,[15] the initial equations, at $\Delta = \Delta_r$, yield $\omega = \text{const}$, $h = \text{const}$, $\Theta_e + \Theta_i = \text{const}$. In this case only the electron and ion temperatures change and their sum remains constant. Behind the shock-wave front, near 2, we have

$$\omega = h = 1, \quad \Theta_e + \Theta_i = 2, \quad (2.8)$$
$$\zeta - \zeta_0 = 0.91\left[\frac{1}{2}\ln\frac{1+\Theta_e^{1/2}}{1-\Theta_e^{1/2}} - \frac{\Theta_e^{3/2}}{3} - \Theta_e^{1/2}\right]. \quad (2.9)$$

Thus, the shock layer produced by the processes of viscosity, dispersion, etc. is followed by a relaxation layer, in which the electron and ion temperatures become equalized. Accurate to small quantities of order Δ/Δ_r, the energy exchange inside the shock layer can be neglected and it can be assumed that the electrons and ions are heated independently.

Returning to the three remaining scales Δ_v, Δ_d, and Δ_j, we note that $\Delta_d \gg \Delta_j \approx \delta\Delta_d$ always. Thus, the principal role in the formation of the shock front is played by the ion viscosity and by the dispersion. The Joule heating and the hole fluxes can appear only as corrections against the background of the dispersion.

The dispersion effects themselves cannot form a shock wave, only oscillations. The damping of these oscillations and the transition from the state 1 into 2 are the result of viscous or Joule dissipations.

Comparing the scales Δ_v and Δ_d, we see that at $M_2^2 \ll (\varepsilon\delta)^{-1}$ ion viscosity predominates—in Fig. 2 this region is marked V. At $M_2^2 \gg (\varepsilon\delta)^{-1}$ the principal process influencing the formation of the shock front is dispersion—region D in Fig. 2. At $\Theta_1^{5/2}(\varepsilon\delta)^{-1} \ll M_2^2 \ll (\varepsilon\delta)^{-1}$ the dispersion at the start of the shock-wave front is more important than the viscosity—the region VD. In the dispersion region, viscous dissipation predominates at $M_2^2 \ll (\varepsilon\delta^2)^{-1}$, and Joule losses are principal at $M_2^2 \gg (\varepsilon\delta^2)^{-1}$—subregions DV and DJ in Fig. 2.

In the region V, as already stated, the principal process influencing the formation of the shock front is ion viscosity.

Substituting $\Delta = l_2/M_2$ in (2.2)–(2.7) we obtain, neglecting terms that are small in ε and δ,

$$\omega - 1 + \frac{3}{10M_2^2}\left(\frac{\Theta_e+\Theta_i}{\omega} - 2\right) + \frac{h^2-1}{2M_{a_2}^2} - \frac{0.32}{\sqrt{10}}\Theta_i^{5/2}\frac{d\omega}{d\zeta} = 0, \quad (2.10)$$

$$\frac{\omega^2-1}{2} + \frac{3}{4M_2^2}(\Theta_e+\Theta_i-2) + \frac{h-1}{M_{a_2}^2} - \frac{0.32}{\sqrt{10}}\Theta_i^{5/2}\omega\frac{d\omega}{d\zeta} = 0, \quad (2.11)$$

$$h\omega - 1 = 0, \quad (2.12)$$

$$\frac{d\Theta_e}{d\zeta} + \frac{2}{3}\frac{\Theta_e}{\omega}\frac{d\omega}{d\zeta} = 0. \quad (2.13)$$

In the entire considered region of variations of M_2, the magnetic field is frozen-in, accurate to terms small in ε and δ [Eq. (2.12)]. The ions are heated on account of the ion viscosity, and the electrons (at the same accuracy) only on account of adiabatic compression. The solution for the profile of the shock-wave front can be obtained in quadratures. We have

$$\Theta_e = \Theta_1(\omega_1/\omega)^{2/3}, \quad (2.14)$$

$$\Theta_i = 2 + \frac{4}{3}(1-\omega) + \frac{10M_2^2}{9}(1-\omega)^2\left(1 - \frac{1}{\omega M_{a_2}^2}\right) - \Theta_e, \quad (2.15)$$

$$\zeta - \zeta_0 = \int_{(1+\omega_1)/2}^{\omega} \frac{0.3\Theta_i^{5/2}(x)\,dx}{(x-1)(x-\omega_1)(x-\omega_-)}. \quad (2.16)$$

The transverse velocity components are small in terms of δ and are given by

$$\lambda_i = -\frac{\delta}{2\sqrt{10}}\frac{\Theta_i}{\omega}\frac{d\omega}{d\zeta}, \quad (2.17)$$

$$\lambda_e = -\frac{\delta}{2\sqrt{10}}\left[\Theta_i + \frac{20M_2^2}{3\omega M_{a_2}^2}\right]\omega\frac{d\omega}{d\zeta}. \quad (2.18)$$

We consider now the region of values of β that are so small that $M_2^2 \gg (\varepsilon\delta)^{-1}$. In this case the scale Δ_d is the largest. We put $\Delta = \Delta_d = \varepsilon\delta M_2 l_2/M_{a2}$. From (2.2)–(2.7) we find that λ_i is small relative to ε, and, omitting small terms in ε, δ^2, and $1/M^2$, we obtain

$$\omega - 1 + \frac{h^2-1}{2M_a^2} - \frac{0.32}{\sqrt{10}}\frac{1}{M^2\varepsilon\delta}\Theta_i^{5/2}\frac{d\omega}{d\zeta} = 0, \quad (2.19)$$

$$\frac{\omega^2-1}{2} + \frac{h-1}{M_a^2} + 0.55\left(\omega\frac{dh}{d\zeta}\right)^2 - \frac{0.32}{\sqrt{10}}\frac{1}{M^2\varepsilon\delta}\Theta_i^{5/2}\omega\frac{d\omega}{d\zeta} = 0, \quad (2.20)$$

$$h\omega - 1 = 1{,}1\omega\frac{d}{d\zeta}\omega\frac{dh}{d\zeta} + 1{,}05\delta\Theta_e^{-3/2}\frac{dh}{d\zeta}. \quad (2.21)$$

Leaving out, in the zeroth approximation, the dissipative terms we have

$$\omega - 1 + (h^2-1)/2M_a^2 = 0, \quad (2.22)$$

$$\frac{\omega^2-1}{2} + \frac{h-1}{M_a^2} + \frac{0.55}{M_a^2}\left(\omega\frac{dh}{d\zeta}\right)^2 = 0, \quad (2.23)$$

$$h\omega - 1 = 1.1\omega\frac{d}{d\zeta}\omega\frac{dh}{d\zeta}. \quad (2.24)$$

Substituting ω from (2.22) in (2.23) and (2.24) and changing over to Lagrangian coordinates by means of the substitution $\omega(d/d\zeta) = (d/d\xi)$, we obtain the following equation for h:

$$\frac{1}{2}\left(\frac{dh}{d\xi}\right)^2 + 0.91\frac{(h-1)^2}{2}\left[\frac{(h+1)^2}{4M_{a_1}^2} - 1\right] = 0, \quad (2.25)$$

$$\frac{d^2h}{d\xi^2} + 0.91(h-1)\left[\frac{h(h+1)}{2M_{a_1}} - 1\right] = 0. \quad (2.26)$$

Equations (2.25) and (2.26) have a well known mechanical analogy,[24,25] namely the energy integral and the equation of motion of a particle of unit mass in the field of a potential $U(h)$.

In the field $U(h)$ there are two equilibrium points $h_1 = 1$ and $h_2 = [-1 + (1 + 8M_{a1}^2)^{1/2}]/2$, corresponding to two singular limiting points corresponding in term to states 1 and 2. The phase curves of (2.26) are shown in Fig. 3. It is obvious that without dissipations no solution in the form of a shock wave can be obtained—it is impossible to go over from 1 to 2. It is therefore necessary to change over in (2.25) and (2.26) to dimensionless variables with respect to the state 1. The solution with the boundary condition $h(1) = 1$ is the soliton

$$h(\xi) = 1 + \frac{2(M_{a_1}^2-1)}{1+M_{a_1}\operatorname{ch}(2\xi(1-M_{a_1}^{-2})^{1/2})}. \quad (2.27)$$

Inside the separatrix that starts with the point $h = 1$ (Fig. 3), periodic solutions are possible around $h = h_2$.

The maximum value of h is

$$h_{max} = 2M_{a_1} - 1. \quad (2.28)$$

Substituting h_{max} in (2.22) and stipulating that $\omega(h_{max}) > 0$, we obtain immediately the known relation[24,25]

$$M_{a_1} < 2, \quad h_{max} < 3.$$

These restrictions, however, do not lead to any new conditions whatever, since it is obvious (see Fig. 2)

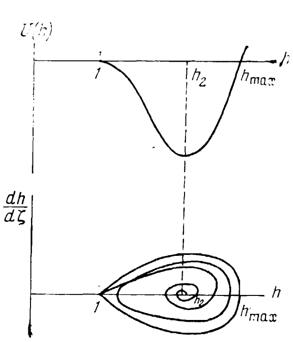

FIG. 3. Form of the function $U(h)$ and the phase curves corresponding to a soliton, a periodic solution, and a shock wave with oscillations that attenuate behind the front.

that at $M_2 \gg 1$ the values of $M_{a_{1,2}}$ differ from unity by a small quantity of the order of $M_2^{-2/3}$. By direct calculations it is easy to find that $M_{a_1} < 2$ already at $M_2 \gtrsim 6$.

We now take into account in the first-order approximation the dissipative terms—the ion viscosity and the Joule losses. Leaving out the small dissipative terms, we have

$$\omega = 1 - \frac{h^2-1}{2M_{a_2}^2} - \frac{1.03}{M_2^2 M_{a_2}^2 \varepsilon\delta} \Theta_i^{5/2} h\omega^{-1} \frac{dh}{d\xi}. \qquad (2.29)$$

Substituting (2.29) in (2.26) we get

$$\frac{d^2h}{d\xi^2} + \frac{1}{\omega}\left[\frac{0.94}{\varepsilon\delta M_2^2 M_{a_2}^2} h^2\Theta_i^{5/2} + 0.95\delta\Theta_e^{-3/2}\right]\frac{dh}{d\xi} + 0.91(h-1)\left[\frac{h(h+1)}{2M_{a_2}^2} - 1\right] = 0. \qquad (2.30)$$

The obtained equation must be solved simultaneously with the heat-conduction equations. Although it is impossible to represent the solution in analytic form, its qualitative character is easily understood.

Linearizing (2.30) near the singular point 2 (i.e., behind the front of the shock wave) as $h \to h_2$, we have

$$\frac{d^2h}{d\xi^2} + 2\gamma\frac{dh}{d\xi} + \Omega^2 h = 0. \qquad (2.31)$$

where

$$\Omega^2 = (3\sqrt{1+8M_{a_2}^2} - 8M_{a_2}^2 - 1)/4M_{a_2}^2 \approx 1 - M_{a_2}^2,$$
$$\gamma = \gamma_v + \gamma_j = 0.94\Theta_i^{5/2}/\varepsilon\delta M_2^2 + 0.95\delta\Theta_e^{-3/2}.$$

We have taken into account here the fact that at $M_2 \gg 1$ we have $M_{a_2} \approx 1$ and $h_2 = \omega_2 = 1$ and the solution of (2.31) is of the form

$$h \sim \exp\left[-(\gamma + i\sqrt{\Omega^2 - \gamma^2})\xi\right]. \qquad (2.32)$$

Obviously, at $\Omega > \gamma$ these are oscillations that attenuate behind the shock-wave front. The quantities γ_v and γ_j determine the relative roles of the ion viscosity and of the Joule heating in the damping of the oscillations. At $(\varepsilon\delta^2)^{-1} \gg M_2^2 \gg (\varepsilon\delta)^{-1}$ the damping is due mainly to ion viscosity, and at $M_2^2 \gg (\varepsilon\delta^2)^{-1}$ to ohmic losses. We note that sufficiently weak shock waves always have a monotonic structure. Indeed, the condition for the existence of oscillations is $\Omega > \gamma_v$ or $\Omega > \gamma_j$. Inasmuch as at $M_2 \gg 1$ we have $M_{a2} \approx 1$, we obtain $\Omega^2 \approx 1 - M_{a_2}^2 \sim I$, where $I \ll 1$ is the shock-wave intensity. We assume $\Theta_i = \Theta_e = 1$ behind the shock-wave front, and then the condition for $\Omega > \gamma_v \times (\Omega > \gamma_j)$ is $I > (\varepsilon\delta M_2^2)^{-2}$ or $I > \delta^2$.

We have already noted that the viscosity effect in the plasma is strong and depends strongly (like $T^{5/2}$) on the temperature; in particular, $\Delta_v(1)/\Delta_v(2) \approx \Theta 1^{5/2}$. Thus, at a large temperature jump the scale that is characteristic of ion viscosity can be much smaller at the beginning of the shock layer than at the end. To the contrary, the dispersion effect, the scale of which is $\Delta_d = c/\omega_p$, does not depend on the temperature. This means that at a large temperature jump in the shock wave (region *VD* in Fig. 2) we can expect the appearance of dispersion effects on the leading edge of the shock-wave front. The velocity and the magnetic field will oscillate near the leading edge, and will subsequently approach monotonically their limiting values in state 2.

Let us consider the shock-wave region with $M_2^2 \ll (\varepsilon\delta)^{-1}$. We write down the equations in Lagrangian coordinates, assuming that $\Delta = \Delta_d = c/\omega_{p_2}$ and omitting terms that are small in ε and δ

$$\omega - 1 + \frac{3}{10M_2^2}\left(\frac{\Theta_i+\Theta_e}{\omega} - 2\right) + \frac{h^2-1}{2M_{a_2}^2} - \frac{0.32}{\sqrt{10}}\frac{\Delta_v}{\Delta_d}\omega^{-1}\Theta_i^{5/2}\frac{d\omega}{d\xi} = 0, \qquad (2.33)$$

$$\frac{\omega^2-1}{2} + \frac{3}{4M_2^2}(\Theta_i+\Theta_e-2) + \frac{h-1}{M_{a_2}^2} + \frac{0.55}{M_{a_2}^2}\left(\frac{dh}{d\xi}\right)^2 - \frac{0.32}{\sqrt{10}}\frac{\Delta_v}{\Delta_d}\Theta_i^{5/2}\frac{d\omega}{d\xi} = 0, \qquad (2.34)$$

$$h\omega - 1 = 1.1\frac{d^2h}{d\xi^2}. \qquad (2.35)$$

In Eqs. (2.33) and (2.34) the terms with the viscosity are multiplied by large factors $\Delta_v/\Delta_d \gg 1$. In the considered case, however, that of a large temperature jump, Θ_i can be arbitrarily small near the lower limit of the shock-wave region in Fig. 2, and consequently the last terms in (2.33) and (2.34) are also small.

To ascertain when oscillations are possible, we put for simplicity

$$\frac{0.32}{\sqrt{10}}\Theta_i^{5/2}\Delta_v/\Delta_d = \lambda = \text{const}.$$

Multiplying (2.33) by ω and subtracting from (2.34) we obtain

$$\Theta_e + \Theta_i = 2 + \frac{4}{3}(1-\omega) + \frac{10M_2^2}{9}(1-\omega)^2 + \frac{10M_2^2}{9M_{a_2}^2}\left[(h-1)^2 + \left(\frac{dh}{d\xi}\right)^2\right]. \qquad (2.36)$$

We linearize the equations in the vicinity of the state 2, putting $h = 1 - x$, $\omega = 1 + y$, $\Theta_i + \Theta_e = 2 - z$ where $x \ll 1$, $y \ll 1$, $z \ll 1$. Then (2.36) yields $z = 4y/3$. Substituting z in the linearized equations (2.33) and (2.35), we get

$$y(1 - M_2^{-2}) - xM_{a_2}^{-2} - \lambda y' = 0, \qquad (2.37)$$
$$x'' - x + y = 0. \qquad (2.38)$$

The characteristic equation of the system (2.37) and (2.38) is

$$\lambda k(k^2-1) - (1 - M_2^{-2})(k^2-1) - M_{a_2}^{-2} = 0. \qquad (2.39)$$

If we neglect viscosity, putting $\lambda = 0$, then at $M_2 \neq 1$ we obtain from (2.39)

$$k^2 + \Omega^2 = 0, \qquad (2.40)$$

where

$$\Omega^2 = [M_2^2/(M_2^2-1) - M_{a_2}^2]/M_{a_2}^2.$$

The quantity $M_{a_2 \max}^2 = M_2^2/(M_2^2 - 1)$ is the upper limit of the variation of $M_{a_2}^2$ in the region of the shock wave (the hyperbola on Fig. 2). At $M_2 > 1$ we always have $\Omega^2 > 0$, i.e., Eq. (2.40) has two conjugate imaginary roots. Consequently, oscillations in the shock-wave profile, due to the dispersion, can arise only at $M_2 > 1$.

We put $\mu = \lambda M_2^2/(M_2^2 - 1)$, then (2.39) takes the form

$$\mu k^3 - \mu k - k^2 - \Omega^2 = 0. \qquad (2.41)$$

It is easy to obtain the critical value of μ, starting with which (2.41) has one real and two imaginary roots

$$\mu_{cr}=\{[1+9\Omega^2+3(9\Omega^4+10\Omega^2+1)^2]^{1/2}-16\}^{1/2}/4\sqrt{3}.$$

Thus, the dispersion becomes appreciable, and oscillations appear on the shock-wave front at $M_2>1$ and

$$\frac{\Delta_v}{\Delta_d}\Theta_1^{5/2}<\mu_{cr}\frac{M_2^2}{M^2-1}. \qquad (2.42)$$

For $M_2\gg1$ we obtain $\Omega^2\approx I\ll1$. Obviously, behind the shock front we have $\Theta_i\approx1$ and $\Delta_v/\Delta_d\gg1$, i.e., the condition (2.42) is not satisfied behind the front. It can be satisfied ahead of the front at a sufficiently small value of Θ_1.

We have already mentioned that the electric field is assumed to be small relative to r_D/Δ and can be obtained in the next-order approximation. From the definition (1.9) it is seen that the jump of the potential

$$\Delta\Phi=\Phi_2-\Phi_1=-(\Delta/r_{D_1})\int_{-\infty}^{+\infty}E(\zeta)\,d\zeta \qquad (2.43)$$

does not depend on the ratio r_D/Δ. The potential difference $\Delta\Phi$ is of interest because it is measured in the experiment. Unlike the discontinuities of all the remaining variables considered by us, the potential jump is determined not by the Hugoniot–Rankine boundary conditions, but by the form of the initial equations, i.e., it depends on the physical processes responsible for the formation of the shock-wave front. Thus, from the measured value of the jump of the potential through the wave front we can, in principle, identify the dominant physical processes and obtain the shock-wave intensity.

In the region V we obtain

$$E=-\frac{5}{3}\frac{r_{D_2}M_2}{l_2\omega}\left[\Theta_e+\frac{3}{10}\Theta_i+\frac{2M_2^2}{\omega M_{a_2}^2}\right]\frac{d\omega}{d\zeta}, \qquad (2.44)$$

$$\Phi_2-\Phi_1=\frac{5M_2^2}{9}\left[\omega_1-1+\left(2+\frac{1}{M_2^2}+\frac{6}{5M_{a_2}^2}\right)\ln\omega_1+\left(1+\frac{3}{M_2^2}+\frac{2}{M_{a_2}^2}\right)\right.$$
$$\left.\times\left(1-\frac{1}{\omega_1}\right)+\frac{5}{2M_{a_2}^2}\left(1-\frac{1}{\omega_1^2}\right)+\frac{63}{50M_2^2}\Theta_1\omega_1^{2/3}(1-\omega_1^{-5/3})\right]. \qquad (2.45)$$

In the region D we have

$$E=-\frac{r_{D_1}}{l_{p_1}}\left[\frac{d}{d\xi}\left(\frac{\Theta_e}{\omega}\right)+\frac{2}{\beta_1}\frac{dh^2}{d\xi}\right], \qquad (2.46)$$

$$\Phi_2-\Phi_1=\frac{\Theta_2}{\omega_2}-1+\frac{2}{\beta_1}\left(\frac{1}{\omega_2^2}-1\right). \qquad (2.47)$$

3. We consider now the shock-wave structure in a completely unmagnetized plasma, i.e., we assume that both $(\Omega_i\tau_i)^{-1}=\delta\gg1$ and $(\Omega_e\tau_e)^{-1}=\varepsilon\delta\gg1$. Let us compare following dissipative terms: the Joule dissipation j^2/σ, the electronic thermal conductivity $d(\varkappa_e dT_e/dx)/dx$, and the ion viscosity $\eta_i(dv/dx)^2$. The electric current is determined from Maxwell's equation $j=(c/4\pi)$ curl $\mathbf{H}$, the coefficient of the electronic thermal conductivity at $\Omega_e\tau_e\ll1$ is $\varkappa_e\approx nT_e\tau_e/m_e$, the conductivity is $\sigma\approx ne^2\tau_e/m_e$, and the ion-viscosity coefficient is $\eta_i\approx nT_i\tau_i$.

Substituting the kinetic coefficient in the dissipative terms and comparing them with one another, we find that the dissipation due to the electronic thermal conductivity is ε^{-1} times larger than that due to ion viscosity (the ionic thermal conductivity is of the same order as the ion viscosity). Comparing the electronic thermal conductivity with the Joule dissipations, we see that their ratio is $\frac{1}{4}\beta_2(\Omega_e\tau_e)^2$. If the last quantity is also small, then the electronic thermal conductivity can be neglected in comparison with the Joule dissipations, which determine the width of the shock-wave front. For numerical values of the temperature expressed in electron volts and of the magnetic field expressed in oersteds, this region will be

$$1.6\cdot10^{-12}nT_{[\mathrm{Oe}]}^{3/2}>H_{[\mathrm{Oe}]}>30T_{[\mathrm{eV}]}^{5/2}.$$

Shock waves with such a range of variation of the plasma parameters are realized in Z pinches and electromagnetic shock tubes, for example at $n\sim10^{15-16}$, $T\sim0.5$–3 eV, and $H\sim0.5$–3 kOe.[26–28]

We substitute in (1.1)–(1.7) the corresponding kinetic coefficient for the unmagnetized plasma. Instead of the last equation of (1.8), it is more convenient to use the equation of the thermal conductivity of the ions

$$\frac{3}{2}C\frac{dT_i}{dx}+nT_i\frac{dv}{dx}+\frac{dq_i}{dx}+\pi_{x\beta}{}^i\frac{dv_\beta{}^i}{dx}=Q_i. \qquad (3.1)$$

Changing over in (1.1)–(1.7) and (3.1) to the dimensionless variables (1.9) we obtain the equations analogous to (2.1)–(2.7) and find the following scales: for the Joule (ohmic) dissipations $\Delta_j=\varepsilon\delta^2Ml/M_a^2$, for the electronic thermal conductivity $\Delta_{T_e}=l/\varepsilon M^3$, for the relaxations connected with the electron–ion heat exchange $\Delta_r=Ml/\varepsilon$, for the ion viscosity and the thermal conductivity $\Delta_{v_i}=l/M$, $\Delta_{T_i}=l/M^3$, and for the electron viscosity $\Delta_{v_e}=\varepsilon l/M$.

Among the foregoing scales, at $\varepsilon\delta\gg1$, the largest is Δ_j, which corresponds to predominance of the ohmic losses. It is therefore natural to choose the scale $\Delta=\Delta_j$ when going to the dimensionless coordinates. Since $\Delta_j\gg\Delta_r$, enough electron–ion collisions can take place over this distance to make $T_i=T_e$ accurate to small quantities of order $\Delta_r/\Delta_j\sim(\varepsilon\delta)^{-2}\ll1$. Indeed, from (3.1) we obtain at $\Delta=\Delta_j$ in terms of the dimensionless variables (1.9)

$$\Theta_e-\Theta_i=O((\varepsilon\delta)^{-2}). \qquad (3.2)$$

We put $\Theta_e=\Theta_i=\Theta$. From (1.3) and (1.5) we have in terms of the dimensionless variables, omitting terms that are small with respect to the parameters ε and $(\varepsilon\delta)^{-1}$

$$\omega-1+\frac{3}{5M_2^2}\left(\frac{\Theta}{\omega}-1\right)+\frac{1}{M_{a_2}^2}(h^2-1)=0, \qquad (3.3)$$

$$\omega^2-1+\frac{3}{M_2^2}(\Theta-1)+\frac{2}{M_{a_2}^2}(h-1)=0. \qquad (3.4)$$

Substituting (1.1) in (1.7) in terms of the variables (1.9) we obtain at $\Delta=\Delta_j$

$$h\omega-1=0.53\Theta_e^{-3/2}\frac{dh}{d\zeta}. \qquad (3.5)$$

Solving (3.3) and (3.4) we obtain h and Θ as functions of ω

$$h=\frac{1}{\omega}+\frac{3}{5\omega}\left\{\left[1+\frac{40M_{a_2}^2}{9}(\omega-1)(\omega_1-\omega)(\omega-\omega_-)\right]^{1/2}-1\right\}, \qquad (3.6)$$

$$\Theta=1-\frac{M_2^2}{3\omega}(\omega-1)(\omega^2+\omega-2/M_{a_2}^2)$$
$$-\frac{2M_2^2}{5\omega M_{a_2}^2}\left\{\left[1+\frac{40M_{a_2}^2}{9}(\omega-1)(\omega_1-\omega)(\omega-\omega_-)\right]^{1/2}-1\right\}, \quad (3.7)$$

where ω_1 is the value of the dimensionless velocity upstream in 1. An expression for ω_1 in terms of M_2 and M_{a_2} is obtained from (1.12) by changing the subscripts $1 \to 2$, while the expression for $\omega_- < 0$ differs from ω_1 in the sign of the square root. The limiting values in the state 2 are $h=\omega=\Theta=1$. From (3.6) and (3.7) we see that h and Θ satisfy all the boundary conditions. Substituting (3.6) and (3.7) in (3.5) and integrating, we obtain

$$\zeta-\zeta_0=0.89\int_{(1+\omega_1)/2}^{\omega}\frac{dh(\omega')}{d\omega'}\Theta^{-1/2}(\omega')\,d\omega'$$
$$\times\left\{\left[1+\frac{40M_{a_2}^2}{9}(\omega'-1)(\omega_1-\omega')(\omega'-\omega_-)\right]^{1/2}-1\right\}^{-1}. \quad (3.8)$$

The lower limit of integration is chosen such that $\omega(\zeta_0)=(1+\omega_1)/2$. Formulas (3.6)–(3.8) solve the problem of the shock-wave structure.

From the Poisson equation and from (1.6) we obtain for the dimensionless electric field and the potential the following expressions:

$$E=-\frac{r_D}{\Delta_j}\left[1.71\frac{d\Theta}{d\omega}-\frac{\Theta}{\omega}+\frac{4.03}{M_{a_2}^2}\omega h\frac{dh}{d\omega}\right]\frac{d\omega}{d\zeta}, \quad (3.9)$$
$$\Phi-\Phi_1=1.71(\Theta-\Theta_1)+\frac{2.02M_2^2}{M_{a_2}^2}\left(\omega h^2-\frac{1}{\omega_1}\right)$$
$$+\int_{\omega}^{\omega_1}\left[\frac{\Theta(\omega')}{\omega'}+\frac{2.02M_2^2}{M_{a_2}^2}h^2(\omega')\right]d\omega'. \quad (3.10)$$

In particular, the jump of the potential through the shock-wave front is

$$\Delta\Phi=\Phi_2-\Phi_1=1.71(1-\Theta_1)+\frac{2.02M_2^2}{M_{a_2}^2}\left(1-\frac{1}{\omega_1}\right)$$
$$+\int_{1}^{\omega_1}\left[\frac{\Theta(\omega')}{\omega'}+\frac{2.02M_2^2}{M_{a_2}^2}h^2(\omega')\right]d\omega'. \quad (3.11)$$

Figure 4 shows the velocity, the magnetic field, the temperature, and the electric variables in the shock wave for $M_1=3$ and $M_{a_1}=2$.

Returning to (3.5), we rewrite it in the form

$$h(\omega)\omega-1=0.53\Theta_c^{-1/2}\frac{dh}{d\omega}\frac{d\omega}{d\zeta}. \quad (3.12)$$

As seen from (3.6), $h>1/\omega$ and consequently, the left-hand side of (3.12) is always positive, i.e., the sign of $d\omega/d\xi$ is determined by the sign of $dh/d\omega$.

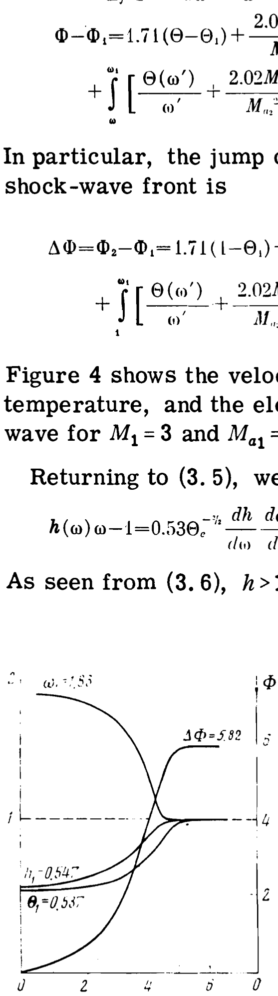

FIG. 4. Structure of shock wave with $M_1^2=9$, $M_{a_1}^2=4$ ($n_1=10^{16}$ cm^{-3}, $T_1=1$ eV, $H_1=1.22\cdot10^3$ Oe).

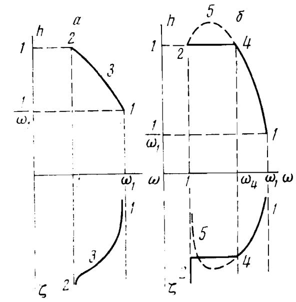

FIG. 5. Plots of $h(\omega)$ and $\omega(\xi)$ for $M_{a_1}<M_{a_1}^h$ (a) and $M_{a_1}>M_{a_1}^h$(b).

In order to investigate the sign of $dh/d\omega$, we eliminate from (3.3) and (3.4) and differentiate the obtained relation once and twice with respect to ω. We have

$$8\omega-5-\frac{3}{M_2^2}+\frac{5(h^2-1)}{2M_{a_2}^2}=\frac{2-5h\omega}{M_{a_2}^2}\frac{dh}{d\omega}, \quad (3.13)$$
$$\frac{5h\omega-2}{M_{a_2}^2}\frac{d^2h}{d\omega^2}+\frac{5\omega}{M_{a_2}^2}\left(\frac{dh}{d\omega}\right)^2+\frac{10}{M_{a_2}^2}h\frac{dh}{d\omega}+8=0. \quad (3.14)$$

Going over to dimensionless variables referred to the state 1 or 2 at these points, we have $h=1$ and $\omega=1$. Taking this into account, we obtain for $dh/d\omega$ at the limiting points 1 and 2

$$\left(\frac{dh}{d\omega}\right)_{1(2)}=-M_{a_{1(2)}}^2\left(1-\frac{1}{M_{1(2)}^2}\right). \quad (3.15)$$

Inasmuch as $M_1>1$ in the shock wave, at the point we always have $dh/d\omega<0$. To the contrary, at the point 2 the inequality $dh/d\omega<0$ is satisfied only for $M_2^2>1$. It can be shown that the solution $M_2^2>1$ is not only necessary but also sufficient for the satisfaction of the inequality $dh/d\omega<0$ at $1<\omega<\omega_1$. This is obvious from the fact that at $M_2^2>1$ at the limiting points 1 and 2 we have $dh/d\omega<0$, and from (3.13) and (3.14) it follows that it is impossible to satisfy simultaneously the conditions $d^2h/d\omega^2>0$ and $dh/d\omega=0$.

Thus, at $M_2^2>1$ we always have $dh/d\omega<0$ at $1<\omega<\omega_1$, and the dependence of h on ω is monotonic (the line 1–3–2 in Fig. 5a), while at $M_2^2<1$ this dependence is represented by the line 1–4–5–2 in Fig. 5b, i.e., there are points where $dh/d\omega>0$. It is obvious from Fig. 5b that the corresponding solution $\omega(\xi)$ is physically unsatisfactory[1)] and it is necessary to introduce an internal discontinuity. It can be shown that in this case the only reasonable path from 1 to 2 satisfying the condition that the entropy must increase is the line 1–4–2 on Fig. 5b. It is natural to use the designation isomagnetic jump for this discontinuity [5, 11, 16, 18]. In an isomagnetic jump, the magnetic field remains constant and all the remaining quantities—the density, velocity, temperature—have discontinuities. In Fig. 6, $M_2^2=1$ corresponds to the line of critical values of the Alfvén Mach numbers $M_a^h\cdot M_a^h=2.76$ as $\beta\to0$. At $1<M_{a_1}<M_{a_1}^h$ a shock-wave front of width on the order of Δ_j is formed on account of Joule dissipations, and at $M_{a_1}>M_{a_1}^h$ an isomagnetic jump should be observed in the structure of the front.

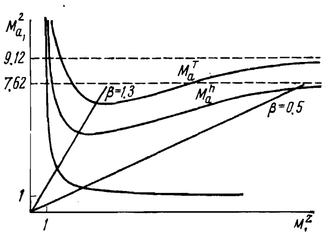

FIG. 6. $M_{a_1}^T$ and $M_{a_1}^h$ are the levels of the critical values of the Alfvén Mach numbers. The straight lines passing through the origin correspond to shock waves with different intensities propagating in a plasma with a specified initial value $\beta_1 = \frac{6}{5} M_{a_1}^2/M_1^2$.

Thus, at $M_{a_1} > M_{a_1}^h$ the Joule dissipations are insufficient for a continuous transition from state 1 to 2, and we must take into account at the location of the discontinuity the dissipations that have a smaller characteristic scale. Since we always have $M_2 \sim 1$ at $M_2^2 < 1$, the scales of the electronic thermal conductivity and of the electron-ion heat exchange are of the same order of magnitude l_2/ε, whereas the ion viscosity and thermal conductivity are small relative to the parameter ε. Neglecting them and introducing on the isomagnetic jump $\Delta = l_2/\varepsilon$, we obtain in analogy with (3.5)

$$dh/d\zeta = O((\varepsilon\delta)^{-2}). \tag{3.16}$$

Thus, in the isomagnetic jump the magnetic field is constant and, as follows from Fig. 5b, is equal to its limiting value $h = 1$ behind the shock-wave front.

To find the structure of the isomagnetic jump, we rewrite (1.3), (1.4), and (3.1) in terms of the variables (1.9), putting $h = 1$, $\Delta = l_2/\varepsilon$ and discarding terms that are small in the parameters,

$$\omega - 1 + \frac{3}{10M_2^2}\left(\frac{\Theta_e+\Theta_i}{\omega} - 2\right) = 0, \tag{3.17}$$

$$\omega^2 - 1 + \frac{3}{2M_2^2}(\Theta_e+\Theta_i-2) - \frac{0.63}{M_2^3}\Theta_e^{5/2}\frac{d\Theta_e}{d\zeta} = 0, \tag{3.18}$$

$$\frac{d\Theta_i}{d\zeta} + \frac{2}{3}\frac{\Theta_i}{\omega}\frac{d\omega}{d\zeta} - \frac{1.9}{M_2}\omega^{-2}\Theta_e^{-3/2}(\Theta_e-\Theta_i) = 0. \tag{3.19}$$

It is seen that the isomagnetic jump is gasdynamic in the sense that the changes of all the quantities in it are determined only by the acoustic Mach number M_2. Consequently, the structure of the isomagnetic jump is analogous to the structure of a shock wave in a plasma without a magnetic field.[29,30] To find the start of the isomagnetic jump (point 4 on Fig. 5b), we substitute $h = 1$ in (3.2) and (3.3) and obtain

$$\omega_4 = \frac{M_2^2+3}{4M_2^2}, \quad \Theta_4 = \frac{(M_2^2+3)(5M_2^2-1)}{16M_2^2}. \tag{3.20}$$

It is convenient to introduce the acoustic Mach number ahead of the isomagnetic jump $M_4 = v_4/u_s(4)$ ($u_s(4)$ is the speed of sound at the point 4). Using (3.20) we obtain

$$M_4^2 = (M_2^2+3)/(5M_2^2-1). \tag{3.21}$$

We note that $M_4^2 > 1$ at $M_2^2 < 1$. From (3.17) and (3.18) we obtain

$$\frac{d\Theta_e}{d\zeta} = 3.16 M_2^3 \Theta_e^{-5/2}(\omega-1)(\omega_4-\omega). \tag{3.22}$$

From (3.22) we see that $(d\Theta_e/d\zeta) > 0$.

Eliminating Θ_i from (3.19), we have

$$\frac{d\omega}{d\zeta} = \left\{3.16 M_2^3\Theta_e^{-5/2}(\omega-1)(\omega_4-\omega) + \frac{3.8}{M_2}\omega^{-2}\Theta_e^{-3/2}\left[\Theta_e - \omega + \frac{5}{3}M_2^2\omega(\omega-1)\right]\right\}\left\{\frac{10}{3} - \frac{10M_2^2}{9}(8\omega-5) - \frac{2}{3}\frac{\Theta_e}{\omega}\right\}^{-1}. \tag{3.23}$$

It is obvious that the first factor in the right-hand side of (3.23) is always positive.

We consider the second factor in (3.23) at the limiting points of the isomagnetic jump 4 and 2 (Fig. 5b), i.e., we put $\Theta_e = 1$ and $\omega = 1$. We see that at the start of the isomagnetic jump we have $d\omega/d\zeta < 0$ at $M_4^2 > \frac{4}{5}$, which is always the case, inasmuch as $d\omega/d\zeta < 0$ at the point 2 only if $M_2^2 > \frac{4}{5}$. Dividing (3.22) by (3.23) we obtain

$$d\Theta_e/d\omega = f(\omega, \Theta_e). \tag{3.24}$$

The form of $\Theta_e(\omega)$ is shown in Fig. 7. At $M_2^2 > \frac{4}{5}$ we have $d\Theta_e/d\omega < 0$ for all $1 < \omega < \omega_4$, and at $M_2^2 < \frac{4}{5}$ the quantity $d\Theta_e/d\omega$ becomes positive and it is necessary to introduce a discontinuity (the 4–4′–3–2 on Fig. 7). In this discontinuity—electron isothermal jump—the density, the velocity, and the temperature of the ions change while the electron temperature and the magnetic field remain constant.

The line $M_2^2 = \frac{4}{5}$ in Fig. 6 represents the critical values the Alfvén Mach number $M_{a_1}^T$. As $\beta \to 0$ we have $M_{a_1}^T = 3.02$. Thus, we should observe in the shock wave a weak isomagnetic jump at $M_{a_1}^T > M_{a_1} > M_{a_1}^h$, and a strong isomagnetic jump with an internal electron isothermal discontinuity at $M_{a_1} > M_{a_1}^T$.

The structure of the weak isomagnetic jump is easy to calculate if it is noted that for $\frac{4}{5} < M_2^2 < 1$ we have $\omega = 1 + x$, where $x \ll 1$, inasmuch as $\omega_{max} = \omega_4 = \frac{19}{16}$ at $M_2^2 = \frac{4}{5}$. Then (3.22) yields

$$\Theta_e^{5/2}\frac{d\Theta_e}{d\zeta} = 3.16 M_2^3 x(x_0 - x), \tag{3.25}$$

where $x_0 = \omega_4 - 1$. From the equation of the thermal conductivity for the ions (3.1) and from the analogous equation (1.8) for the electrons it follows that non-adiabaticity takes place only in third order in x, whence

$$\Theta_i = \Theta_e = \omega^{-2/3} = 1 - {}^2/_3 x + {}^5/_9 x^2. \tag{3.26}$$

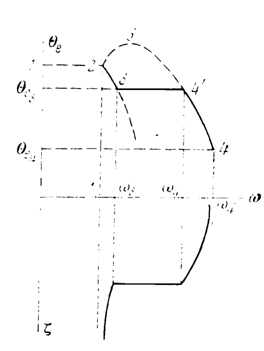

FIG. 7. Plots of $\Theta_e(\omega)$ and $\omega(\zeta)$ for $M_{a_1} > M_{a_1}^T$ and $M_2^2 < \frac{4}{5}$.

Integration of (3.25) and (3.26) accurate to second order in x yields

$$\omega=1+\frac{\omega_4-1}{1+\exp[4.74M_2^3(\omega_4-1)(\zeta-\zeta_0)]}. \qquad (3.27)$$

The width of the weak isomagnetic jump in accord with Prandtl is

$$\Delta_4\approx\frac{0.56}{M_2(1-M_2^2)}\frac{l_2}{\varepsilon}. \qquad (3.28)$$

In the general case the width of the isomagnetic jump is the characteristic length of the electronic thermal conductivity l_2/ε. For the electric field, for the potential, and for its change $\Delta\Phi$ over a weak isomagnetic jump we obtain

$$E=\frac{\varepsilon r_{D_2}}{l_2}\left[1.71\frac{d\Theta_e}{d\zeta}-\frac{\Theta_e}{\omega}\frac{d\omega}{d\zeta}\right]=-2.14\frac{\varepsilon r_{D_2}}{l_2}\omega^{-5/3}\frac{d\omega}{d\zeta}, \qquad (3.29)$$

$$\Phi-\Phi_4=3.21(\omega^{-2/3}-\omega_4^{-2/3});\quad \Delta\Phi=3.21(1-\omega_4^{-2/3}). \qquad (3.30)$$

Figure 8 shows the changes of h, ω, Θ, and Φ in a shock wave with weak isomagnetic jumps.

At $M_2^2<\frac{4}{5}$ or $M_{a_1}>M_{a_1}^T$, as we have seen, it is necessary to introduce inside the isomagnetic jump an electron isothermal discontinuity, the structure of which is determined by the viscosity and thermal conductivity of the ions. Its isothermal character follows from (1.5) at $\Delta=l_2$ (in complete analogy with (3.16)). If Θ_e is constant, Eq. (3.1) can be integrated with the aid of (1.3). The structure of this jump is determined by the following equations:

$$\omega-1+\frac{3}{10M_2^2}\left(\frac{\Theta_i+\Theta_e}{\omega}-2\right)-\frac{0.404}{M_2}\Theta_i^{5/2}\frac{d\omega}{d\zeta}=0, \qquad (3.31)$$

$$\frac{5}{3}M_2^2\omega^2-2\left(\frac{5}{3}M_2^2+1\right)\omega+\frac{2}{3}\Theta_i+\Theta_e\ln\omega+\frac{0.276}{M_2}\Theta_i^{5/2}\frac{d\Theta_i}{d\zeta}=K. \qquad (3.32)$$

Here K is an integration constant determined from the boundary conditions.

The electron isothermal jump is quite similar in structure to the shock layer in a magnetized plasma—in both cases the role of the principal dissipation is played by ion viscosity, which forms a monotonic profile of the shock front; no restrictions whatever are imposed on the shock-wave intensity, since the viscosity is capable of ensuring any required dissipation.

The solution for a shock wave with an isomagnetic jump of arbitrary intensity ($M_{a_1}>M_{a_1}^T$) is given in the general case by formulas (3.6)–(3.8) for $\omega_4<\omega<\omega_1$, by combined numerical integration of Eqs. (3.22) and (3.23) at $\omega_4'<\omega<\omega_4$, and by (3.31) and (3.32) inside the electron isothermal jump (Fig. 9).

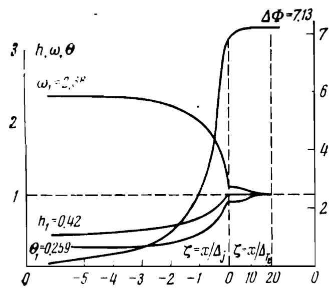

FIG. 8. Structure of shock wave with weak isomagnetic jump $M_1^2=20$, $M_{a_1}^2=7$ ($n_1=10^{16}$ cm^{-3}, $T_1=1$ eV, $H_1=1.38\cdot10^3$ Oe). The scale of the isomagnetic jump has been stretched out for clarity.

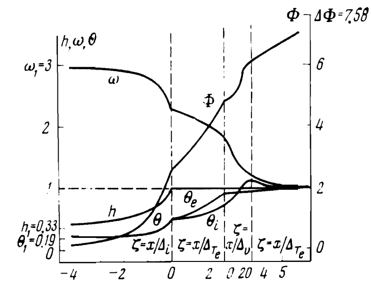

FIG. 9. Structure of shock wave with strong isomagnetic jump. $M_1^2=17$, $M_{a_1}^2=25$ ($n_1=10^{16}$ cm^{-3}, $T_1=1$ eV, $H_1=6.75\cdot10^2$ Oe). The scales of the isomagnetic and electron isothermal jumps have been stretched out for clarity.

An investigation of the Hugoniot conditions for Eqs. (3.31) and (3.32) shows that the electron isothermal jump divides the isomagnetic jump into two parts. If the isomagnetic jump is strong ($M_4\gg1$), then in its first part the quantity that increases mainly is the electron temperature (to a value close to the limit), and then in the isothermal jump abrupt changes take place in the velocity and the ion temperature (which becomes higher than the limiting value); in the remaining part, owing to the electronic thermal conductivity, there is a slight decrease in the velocity and an increase in the temperature of the electrons, and in addition the ions give up heat to the electrons, and their temperatures become equalized. If we consider shock waves with fixed initial state (in which the plasma is weakly magnetized), then with increasing intensity an ever increasing part of the total jump of the density, temperature, or potential is reached in the isothermal jump. Recognizing also that a sufficiently strong wave makes the plasma magnetized, we can conclude that the structure of these strong shock waves differs from that considered in Sec. 2 only in the relatively small Joule section in the leading part of the shock front.

The jump of the potential through the isomagnetic discontinuity is calculated in the same manner as before. Ahead and behind the isothermal discontinuity we have

$$\Phi-\Phi_4'=1.71(\Theta_e-\Theta_4')+\int_{\omega}^{\omega_4'}\frac{\Theta_e(\omega')}{\omega'}d\omega', \qquad (3.33)$$

$$\Phi-\Phi_4=1.71(\Theta_e-\Theta_4)+\int_{\omega}^{\omega_4}\frac{\Theta_e(\omega')}{\omega'}d\omega'. \qquad (3.34)$$

In the isothermal discontinuity the potential varies in accordance with

$$\Phi-\Phi_3=\Theta_{e_3}\ln\frac{\omega_3}{\omega}. \qquad (3.35)$$

4. Finally, we consider briefly one more limiting case, which has a much narrower applicability in comparison with that considered above. This is the intermediate case of a partly magnetized plasma, when the

electrons are magnetized ($\Omega_e \tau_e \gg 1$), and the ions are not magnetized ($\Omega_i \tau_i \ll 1$). Obviously, this state will be preserved behind the front only in the case of a very small temperature jump. Changing over in (1.1)–(1.8) to the dimensionless variables (1.9), we find that in this case the main dissipations will be the Joule losses and the electronic thermal conductivity (the respective scales are $\Delta_j = \varepsilon\delta^2 Ml/M_a^2$ and $\Delta_{T_e} = \varepsilon\delta^2 l/M^3$), and the ion viscosity and the thermal conductivity will be small ($\Delta_{v_i} = l/M$, $\Delta_{T_i} = l/M^3$), if we stipulate that all the Mach numbers be of the order of unity and the inequality $\varepsilon\delta^2 \gg 1$ is satisfied. It is easy to show that only when the foregoing conditions are satisfied does the limit of a partially magnetized plasma have a qualitatively distanct behavior, and the corresponding solutions are different from those considered above. Choosing $\Delta = \Delta_j$, we obtain the equations of the shock layer

$$\omega - 1 + \frac{3}{10M_2^2}\left(\frac{\Theta_i+\Theta_e}{\omega} - 2\right) + \frac{1}{2M_{a_2}^2}(h^2-1) = 0, \tag{4.1}$$

$$\frac{\omega^2-1}{2} + \frac{3}{4M_2^2}[\Theta_i+\Theta_e-2) + \frac{1}{M_{a_2}^2}(h-1)$$
$$-\frac{4.5}{\sqrt{10}}\omega^{-1}\Theta_e^{-1/2}h^{-1}\frac{dh}{d\zeta} - \frac{4.66M_{a_2}^2}{(\sqrt{10}/3)^{3/2}M_2^4}\omega^{-2}h^{-2}\Theta_e^{-1/2}\frac{d\Theta_e}{d\zeta} = 0, \tag{4.2}$$

$$h\omega - 1 = \frac{\sqrt{10}}{3}\Theta_e^{-3/2}\frac{dh}{d\zeta} + \frac{4.5M_{a_2}^2}{\sqrt{10}M_2^2}\omega^{-1}h^{-1}\Theta_e^{-3/2}\frac{d\Theta_e}{d\zeta}, \tag{4.3}$$

$$\frac{3}{2}\frac{d\Theta_i}{d\zeta} + \frac{\Theta_i}{\omega}\frac{d\omega}{d\zeta} = 0. \tag{4.4}$$

Equation (4.4) can be immediately integrated and yields

$$\Theta_i = s\omega^{-2/3}. \tag{4.5}$$

The integration constant s in (4.5) is determined by the boundary condition $T = T_1$ at $v = u_1$; if we change in the system (4.2)–(4.4) to dimensionless variables relative to state 1 or 2, this yields respectively $s = 1$ or $s = \Theta_1 \omega_1^{2/3}$.

From (4.1) we can express Θ_e in terms of ω and h, after which the system reduces to the two equations

$$\frac{d\omega}{d\zeta} = \left\{1.31\Theta_e(1-h\omega) - 0.69h\omega M_2^2\left[2(\omega-\omega_4)(\omega-1) + \frac{(h-1)(5h\omega+5\omega-4)}{4M_{a_2}^2}\right]\right\}A^{-1}(h,\omega), \tag{4.6}$$

$$\frac{dh}{d\zeta} = \frac{\sqrt{10}}{3}\Theta_e^{1/2}\left\{0.62h\omega M_2^2\left[2(\omega-\omega_4)(\omega-1) + \frac{(h-1)(5h\omega+5\omega-4)}{4M_{a_2}^2}\right] - 0.57\Theta_e(1-h\omega)\right\}, \tag{4.7}$$

where

$$A(h,\omega) = \frac{3M_{a_2}^2}{\sqrt{10}M_2^2}\omega^{-1}h^{-1}\Theta_e^{-1/2}\left[\frac{20M_2^2}{3}\omega - \frac{10M_2^2}{3} - 2 - \frac{2}{3}s\omega^{-5/3} + \frac{5M_2^2}{3M_{a_2}^2}(h^2-1)\right].$$

The situation here is analogous to that in the investigation of the system (3.22) and (3.23). We must determine the sign of $A(h, \omega)$—the denominator of the right-hand side of (4.6).

If this sign is different at points 1 and 2, then the denominator vanishes on the integral curve leading from 1 to 2, meaning ambiguity of $\omega(\xi)$, i.e., a physically meaningless solution. It is easily seen that at the point 1 we always have $A(h, \omega) > 0$. After the point 2, here $A > 0$ only if $M_2^2 > M_{2_{cr}}$, where $M_{2_{cr}}$ is the solution of the transcendental equation

$$M_2^2 = (3+\Theta_1\omega_1^{2/3})/5. \tag{4.8}$$

Here Θ_1 and ω_1 are expressed in terms of M_2^2 and $M_{a_2}^2$ with the aid of (1.12) and (1.13) with the interchange of the subscripts $1 \leftrightarrow 2$. Equation (4.8) determines the line of the critical Mach numbers on the plane (M_2^2, $M_{a_2}^2$) (or (M_1^2, $M_{a_1}^2$)). In the limit as $\beta \to 0$ we can determine analytically the value of the critical Alfvén Mach number, noting that this limit corresponds to the lower limit of the shock-wave region in Fig. 2, on which $\Theta_1 = 0$, i.e., $M_{2_{cr}}^2 = \frac{3}{5}$. Simple calculation with the aid of the parametric equations of this lower limit and (1.11) yield

$$M_{a_1{cr}} = 2\cdot 3^{1/2} \approx 3.46. \tag{4.9}$$

On the other hand, if the Alfvén Mach number exceeds the critical value, then it is necessary to introduce an internal discontinuity. Assuming $\Delta = l_2$, in exactly the same way in the foregoing analysis of the isothermal and isomagnetic discontinuities, we find that this jump, accurate to small quantities of order $(\varepsilon\delta^2)^{-1}$, is simultaneously isomagnetic and isothermal with respect to the electrons. Since it already includes the ion viscosity, the problem has no other critical numbers or internal jumps.

We do not investigate this limiting case in greater detail, because the larger the temperature jump, the more difficult it is to satisfy the conditions indicated at the start of this section; this is impossible even in principle in the limit of the infinitely large temperature jump needed for the derivation of (4.9). Therefore the analysis undertaken in this section is more readily of formal interest. This completes the inquiry into the physical situations that correspond in a collision-dominated plasma to different critical Mach numbers, which are well known in the limit as $\beta \to 0$[10]; in particular, it can be concluded that (4.9) does not seem to have any physical meaning.

We note in conclusion that since we calculate the structure of the shock wave by using the equations of two-fluid hydrodynamics, all the results are meaningful, of course, only in the range of variation of the plasma parameters where these equations are valid, although, as shown in[31], the use of the Navier–Stokes and Fokker–Planck equations give very close results. In the case of a nonmagnetized plasma, inasmuch as the width of the shock-wave front is much larger than the mean free path, the hydrodynamic approximation is certainly correct. On the other hand, when $\Omega_i \tau_i \gg 1$, the ions do not have time to become Maxwellized on the shock-wave front, and in this sense the use of the hydrodynamic equations is more readily model-dependent.

The authors thank academician P. L. Kapitza for useful remarks, academician Ya. B. Zel'dovich, Professor L. P. Pitaevskiĭ, and Professor S. I. Anisimov for a discussion of the results.

[1)]It can be shown that $d\theta/d\xi < 0$ at $dh/d\omega > 0$, but this is impossible in a shock wave.

[1]C. K. Chu and R. Grass, in: Physics of Hot Plasmas, Adv. in Plasma Physics, Vol. 2, Wiley-Interscience, N.Y. 1969.
[2]A. G. Kulikovskiĭ and G. A. Lyubimov, Magnitnaya gidrodinamika (Magnetohydradynamics), Fizmatgiz, 1962.
[3]Ya. B. Zel'dovich, Zh. Eksp. Teor. Fiz. 32, 1126 (1957) [Sov. Phys. JETP 5, 919 (1957)].
[4]V. D. Shafranov, Zh. Eksp. Teor. Fiz. 34, 1475 (1958) [Sov. Phys. JETP 7, 1019 (1958)].
[5]W. Marshall, Proc. R. Soc. Lond. A233, 367 (1955).
[6]R. Jourdan, Plasma Phys. 11, 57 (1969).
[7]H. K. Sen, Phys. Rev. 102, 5 (1956).
[8]S. H. Schneider, Phys. Fluids 15, 805 (1972).
[9]R. T. Taussig, Phys. Fluids 16, 384 (1973).
[10]L. S. Woods, Plasma Phys. 11, 25 (1969).
[11]G. A. Lyubimov, Fiz. Metal. Metalloved. 25, 179 (1961).
[12]T. P. Coffey, Phys. Fluids 13, 1249 (1970).
[13]P. N. Hu, Phys. Fluids 9, 89 (1966).
[14]P. N. Hu and H. Grad, Phys. Fluids 10, 2597 (1967).
[15]A. L. Velikovich and M. A. Liberman, Fiz. Plazmy 2, 334 (1976) [Sov. J. Plasma Phys. 2, 182 (1976)].
[16]L. D. Landau and E. M. Lifshitz, Mekhanika sploshnykh sred (Fluid Mechanics), Fizmatgiz, 1954, p. 88 [Pergamon, 1958].
[17]V. S. Imshennik, Zh. Eksp. Teor. Fiz. 42, 236 (1962) [Sov. Phys. JETP 15, 167 (1962)].
[18]V. A. Belokon', Zh. Eksp. Teor. Fiz. 36, 341 (1959) [Sov. Phys. JETP 9, 235 (1959)].
[19]V. A. Belokon', *ibid.*, 1316 [932].
[20]L. S. Woods, J. Plasma Phys. 3, 435 (1969).
[21]J. W. M. Paul, M. J. Parkinson, J. Sheffield, and L. S. Holmes, Nature (Lond.) 208, 133 (1968).
[22]V. G. Eselevich, A. G. Es'kov, R. Kh. Kurtmullaev, and A. I. Malyutin, Zh. Eksp. Teor. Fiz. 60, 2079 (1971) [Sov. Phys. JETP 33, 1120 (1971)].
[23]S. I. Braginskiĭ, Voprosy teoriya plazmy (Problems of Plasma Theory), Vol. 1, Atomizdat, 1962.
[24]R. S. Sagdeev, *ibid.*, Vol. 4, Atomizdat, 1964.
[25]V. I. Kariman, Nelineĭnye volny v dispergiruyushchikh sredakh (Nonlinear Waves in Dispersive Media), Nauka, 1973.
[26]A. D. Craig, Plasma Phys. 17, 1111 (1975).
[27]D. H. McNeil, Phys. Fluids 18, 44 (1975).
[28]S. V. Bazdenkov and V. V. Vikhrev, Fiz. Plazmy 1, 451 (1975) [Sov. J. Plasma Phys. 1, 250 (1975)].
[29]V. S. Imshennik, Zh. Eksp. Teor. Fiz. 42, 236 (1962) [Sov. Phys. JETP 15, 167 (1962)].
[30]M. Y. Jaffrin and R. T. Probstein, Phys. Fluids 1, 1658 (1964).
[31]K. Abe, Phys. Fluids 18, 1125 (1975).

Translated by J. G. Adashko

Instability and self-refraction of solitons

L. A. Ostrovskiĭ and V. I. Shrira

Scientific-Research Institute of Radiophysics

(Submitted May 4, 1976)
Zh. Eksp. Teor. Fiz. 71, 1412–1420 (October 1976)

The nonlinear evolution of a two-dimensional soliton with a nonplanar front is investigated in terms of the ray theory. A necessary condition for the stability of an arbitrary soliton in isotropic and anisotropic media is obtained. It turns out that stability is enhanced by anisotropy and that cylindric convergence of the front leads to instability in some cases and to asymptotic stability of the soliton in other cases. The nonlinear stage of self-refraction of the converging and diverging parts of the front is considered. Because of nonlinear defocusing, the field in the focus of a converging soliton remains finite and a cylindric front becomes plane. This is followed by the appearance of a sharp break on the front and a "shock-soliton" type singularity, leading to the destruction of the soliton. General results are applied to the analysis of the behavior of solitons in media with different degrees of nonlinearity.

PACS numbers: 42.65.–k

1. THE GEOMETRIC OPTICS OF SOLITONS

Most problems concerned with nonlinear solitary waves, i.e., solitons, have so far been solved in the one-dimensional formulation. At the same time, the essential point for many physical situations is that the soliton is a "wave layer" moving in space, which may not be strictly plane, and the soliton parameters will, in general, vary along the layer. Kadomtsev and Petviashvili[1] have discussed small deformations of the plane front of a soliton, and have shown that it may become unstable within the framework of the two-dimensional generalization of the Korteweg and de Vries equation. Some nonlinear solutions of this equation were subsequently obtained in[2].

A very effective approach to the solution of two- and three-dimensional problems involving solitons can be developed within the framework of nonlinear geometric optics. This involves the consideration of the variation of amplitude and velocity of a soliton along ray tubes defined by the normals to the soliton front, the local velocity of which depends on the amplitude. This method has already been used to consider the propagation of cylindrically and spherically symmetric solitons and the refraction of solitons in an inhomogeneous medium.[3,4] This analysis was, however, performed in the linear ray-optics approximation when nonlinearity did not affect the distribution of rays even though it was important for the evolution of the wave along the ray tubes. To investigate nonlinear self-refraction effects (which are fundamentally related to the possibility of instability), it is necessary to write down the coupled equations for the ray paths and for the variation of the soliton ampli-